AFRL-RX-WP-TR-2010-4183

COLLABORATIVE RESEARCH AND DEVELOPMENT (CR&D)

Delivery Order 0067: Molecular Simulations for Hydrated Polymer Fuel Membranes

James C. Moller

Universal Technology Corporation

NOVEMBER 2007
Final Report

AIR FORCE RESEARCH LABORATORY
MATERIALS AND MANUFACTURING DIRECTORATE
WRIGHT-PATTERSON AIR FORCE BASE, OH 45433-7750
AIR FORCE MATERIEL COMMAND
UNITED STATES AIR FORCE

NOTICE AND SIGNATURE PAGE

Using Government drawings, specifications, or other data included in this document for any purpose other than Government procurement does not in any way obligate the U.S. Government. The fact that the Government formulated or supplied the drawings, specifications, or other data does not license the holder or any other person or corporation; or convey any rights or permission to manufacture, use, or sell any patented invention that may relate to them.

This report was cleared for public release by the USAF 88th Air Base Wing (88 ABW) Public Affairs Office (PAO) and is available to the general public, including foreign nationals. Copies may be obtained from the Defense Technical Information Center (DTIC) (http://www.dtic.mil).

AFRL-RX-WP-TR-2010-4183 HAS BEEN REVIEWED AND IS APPROVED FOR PUBLICATION IN ACCORDANCE WITH THE ASSIGNED DISTRIBUTION STATEMENT.

*//Signature//	//Signature//
MARK GROFF Program Manager Business Operations Branch Materials & Manufacturing Directorate	KENNETH A. FEESER Branch Chief Business Operations Branch Materials & Manufacturing Directorate

This report is published in the interest of scientific and technical information exchange, and its publication does not constitute the Government's approval or disapproval of its ideas or findings.

*Disseminated copies will show "//Signature//" stamped or typed above the signature blocks.

REPORT DOCUMENTATION PAGE

Form Approved
OMB No. 0704-0188

1. REPORT DATE *(DD-MM-YY)*	2. REPORT TYPE	3. DATES COVERED *(From - To)*
November 2007	Final	07 December 2006 – 01 August 2007

4. TITLE AND SUBTITLE
COLLABORATIVE RESEARCH AND DEVELOPMENT (CR&D)
Delivery Order 0067: Molecular Simulations for Hydrated Polymer Fuel Membranes

5a. CONTRACT NUMBER
F33615-03-D-5801-0067

5b. GRANT NUMBER

5c. PROGRAM ELEMENT NUMBER
62102F

6. AUTHOR(S)
James C. Moller

5d. PROJECT NUMBER
4349

5e. TASK NUMBER
L0

5f. WORK UNIT NUMBER
4349L0VT

7. PERFORMING ORGANIZATION NAME(S) AND ADDRESS(ES)
Universal Technology Corporation
1270 North Fairfield Road
Dayton, OH 45432-2600

8. PERFORMING ORGANIZATION REPORT NUMBER
S-531-067

9. SPONSORING/MONITORING AGENCY NAME(S) AND ADDRESS(ES)
Air Force Research Laboratory
Materials and Manufacturing Directorate
Wright-Patterson Air Force Base, OH 45433-7750
Air Force Materiel Command
United States Air Force

10. SPONSORING/MONITORING AGENCY ACRONYM(S)
AFRL/RXOB

11. SPONSORING/MONITORING AGENCY REPORT NUMBER(S)
AFRL-RX-WP-TR-2010-4183

12. DISTRIBUTION/AVAILABILITY STATEMENT
Approved for public release; distribution unlimited.

13. SUPPLEMENTARY NOTES
PAO Case Number: 88ABW 2010-1198; Clearance Date: 16 Mar 2009. Report contains color.

14. ABSTRACT
This research in support of the Air Force Research Laboratory Materials and Manufacturing Directorate was conducted at Wright-Patterson AFB, Ohio from 7 December 2006 through 1 August 2007. The effects of hydration level and temperature on solvent dynamics and nano-structural morphology for two polymers which show promise as membranes in polymer electrolyte fuel cells; sulfonated poly (thioether sulfone) (SPTES) and Nafion-117 were studied via molecular dynamics simulations. Solvent molecule behavior was characterized and examined according to proximity to polar side groups on the respective polymer chains. In addition to solvent linear diffusion and molecule vector rotation analysis, velocity autocorrelation was used to identify oscillatory molecule motions. Hydrogen bonding among solvent molecules and with polar groups was identified according to geometric criteria. It was found that these bonds are amenable to proton transfer.

15. SUBJECT TERMS
polymer electrolyte fuel cells

16. SECURITY CLASSIFICATION OF:			17. LIMITATION OF ABSTRACT:	18. NUMBER OF PAGES	19a. NAME OF RESPONSIBLE PERSON (Monitor)
a. REPORT	b. ABSTRACT	c. THIS PAGE			Mark Groff
Unclassified	Unclassified	Unclassified	SAR	30	19b. TELEPHONE NUMBER *(Include Area Code)* N/A

Standard Form 298 (Rev. 8-98)
Prescribed by ANSI Std. Z39-18

FINAL REPORT

Contractor :	James C. Moller
Reporting Period :	Summer 2007
Prime Contract :	F33615-03-D-5801
Independent Contractor Agreement :	07-S531-067-C1
Title :	Molecular Simulations for Hydrated Polymer Fuel Cells

ABSTRACT

The effects of hydration level and temperature on solvent dynamics and nano-structural morphology for two polymers which show promise as membranes in polymer electrolyte fuel cells; sulfonated poly (thioether sulfone) (SPTES) and Nafion-117 were studied via molecular dynamics simulations. Solvent molecule behavior was characterized and examined according to proximity to polar side groups on the respective polymer chains. In addition to solvent linear diffusion and molecule vector rotation analysis, velocity autocorrelation was used to identify oscillatory molecule motions. Hydrogen bonding among solvent molecules and with polar groups was identified according to geometric criteria. It was found that these bonds are amenable to proton transfer.

1. INTRODUCTION

While polymer electrolyte membrane fuel cells (PEMFCs) hold out the possibility for providing several important benefits as power sources, there are several technical hurdles which need to be surmounted in order for them to provide service in common applications. Among the broader aims of the research is to develop PEMFC systems which can operate at higher temperatures than presently achievable while still maintaining sufficiently high proton conductivity in the hydrated membrane. The operating temperature needs to high enough to avoid electrode contamination but low enough to avoid boiling the electrolyte solution. Various strategies for surmounting the barrier have included alterations in the polymer chain structure and polar groups, using various acids as substitutes for water, and the addition of proton-conductive inorganic substances and polymers.

A great deal is known thus far regarding chemical dynamics and morphology within membranes (1). Various modeling (2-4) and experimental efforts have provided insight into the mechanisms which enable proton conduction in PEMFCs. Hydrated membranes are two-phase systems, an interconnected system of water-filled pores and a network of fibrils (5,6). Water solvates the polar groups and clustering of water molecules at the groups excludes protons. This is thought to contribute to the mobility of protons via both vehicular (7) and hopping (8,9)

mechanisms. Deprotonation of the acidic group is predicted to create sites other than the polar groups which also are stable sites for water molecules (10).

Among the most common PEM candidate materials are polymers with polytetrafluoroethylene backbones and short perfluorosulfonic acid side chains. DuPont Nafion is the example most commonly studied. The Nafion variant investigated here is shown in Figure 1a. More recently, polymers with aromatic backbones and acidic side groups have been synthesized and demonstrated to have high conductivity at elevated temperatures (11,12). The molecule from this class which was investigated here, sulfonated poly (thio ether sulfone) (SPTES), is shown in Figure 1b.

The overarching aim of the effort reported here was to investigate solvent mobility vis-à-vis experimental results. In particular, the geometric and dynamical factors which affected solvent rotational mobility in molecular dynamics simulations were studied.

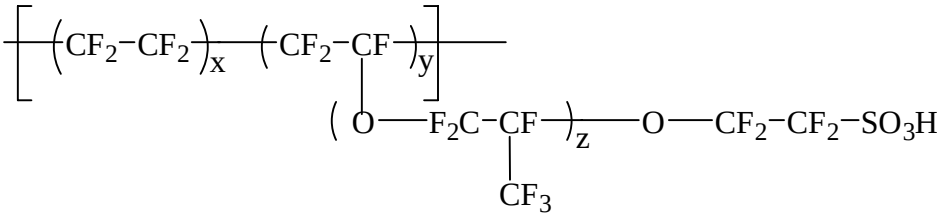

a)

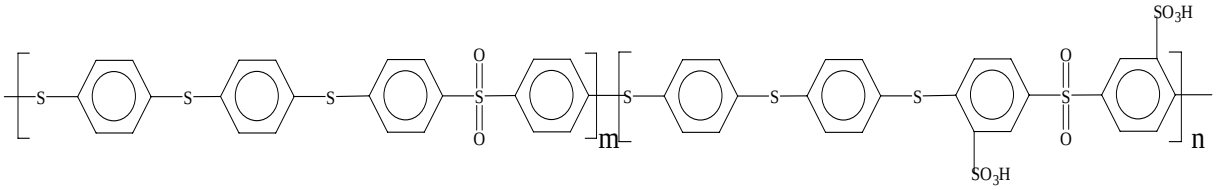

b)

Figure 1. Renderings the SPTES (a) and Nafion (b) molecules.

2. ATOMISTIC SIMULATIONS

Simulations of hydrated SPTES and Nafion 117 systems were performed. Due to the strong dependence of transport and nanostructure upon them, hydration level and temperature were the principal variables. The systems are summarized in Tables 1. In the SPTES systems, the degree of sulfonation (DS) was also varied because it is thought that hydrated system mechanical strength and solvent diffusion rates vary inversely with each other as DS varies. DS is defined by

$$DS = \frac{n}{m+n} \times 100$$

SPTES systems contained four five-unit chains. Nafion systems included four ten-unit chains and where $x = 7$, $y = 1$, and $z = 1$ (as shown in Figure 1a). Hydronium molecules were used to counter the charge on the deprotonated sulfonate groups and permit some proton mobility. The ESFF force field (13) was used for both systems. Point charges on hydronium nuclei, polar groups, and phenyl rings were altered to more closely match those obtained by quantum density functional theory calculations. The charges are given in Table 2 and Figure 2. Systems were equilibrated under isobaric-isothermal conditions in increments of 50^o K. Canonical ensemble runs were performed for several nanoseconds at each temperature.

DS	λ = Solvent molecules/SO_3	Water molecules	Hydronium molecules	Total atoms	Cell size (A) (at 300^o K)
40	6	80	16	1452	26.3
"	9	128	"	1596	26.5
60	6	120	24	1628	26.6
"	9	192	"	1844	27.6
"	12	264	"	2060	28.0
"	15	336	"	2276	28.7
80	6	160	32	1804	26.9
100	6	200	40	1980	27.7

a)

λ	Water molecules	Hydronium molecules	Total atoms	Cell size (A) (at 300^o K)
6	200	40	3488	35.2
15	560	40	4568	37.7
24	920	40	5648	40.0

b)

Table 1. Summaries of the SPTES (a) and Nafion (b) systems.

Molecule	*Atom*	*Point Charge*
Water		
	H	0.40
	O	-0.80
Hydronium		
	H	0.461
	O	-0.382

Table 2. Summary of point charges assigned to water and hydronium atoms.

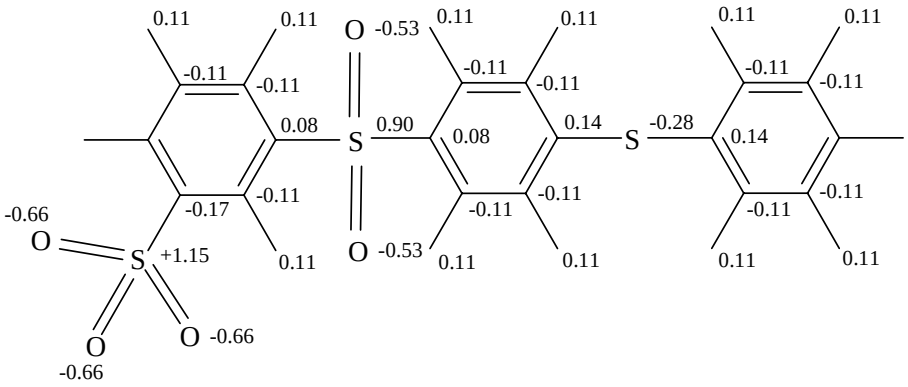

Figure 2. Summary of point charges assigned to sulfonate, sulfone, and phenyl groups in simulations of SPTES

3. RESULTS & DISCUSSION

3.1 Solvent Bound State

It is frequently found that, in the presence of polar groups such as the acidic pendant groups found in both Nafion and SPTES, solvent molecule dynamics and ordering is strongly dependent on proximity to these groups. In the context of anticipating fuel cell membrane performance, it is thought that understanding behaviors among these groups is essential. Therefore, in much of the following analyses, the solvent molecule population was sorted according to this proximity. Molecules having their center-of-mass within the first solvation shell of the acidic group were termed *bound*, molecules having only non-bound solvent molecules as immediate neighbors were termed *free*, and the remaining molecules were classed as *loosely-bound*.

The relative fractions of bound, loosely-bound, and free water and hydronium were examined. The dependence of these on temperature and hydration level are shown in Figure 3. It is found that the hydronium remains largely in the free state for $\lambda > 6$ and that the amount of

bound water reaches a level of approximately 5.5 water molecules in the first salvation shell. Any additional water principally resides in the bound state.

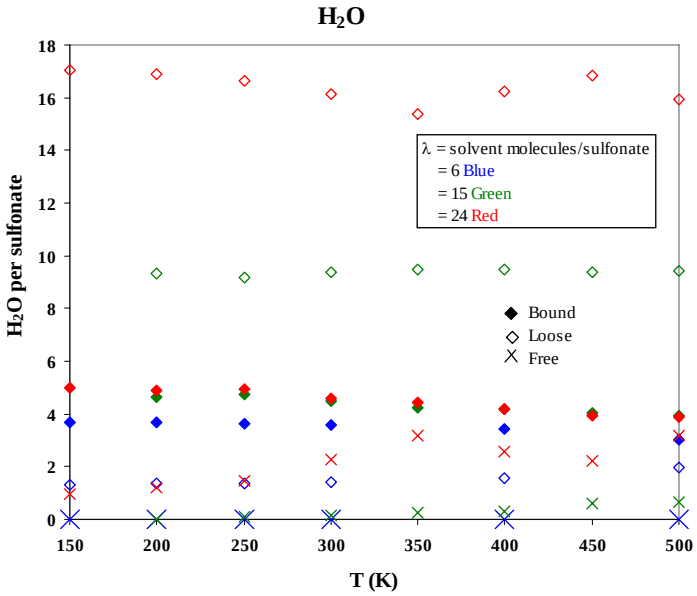

a)

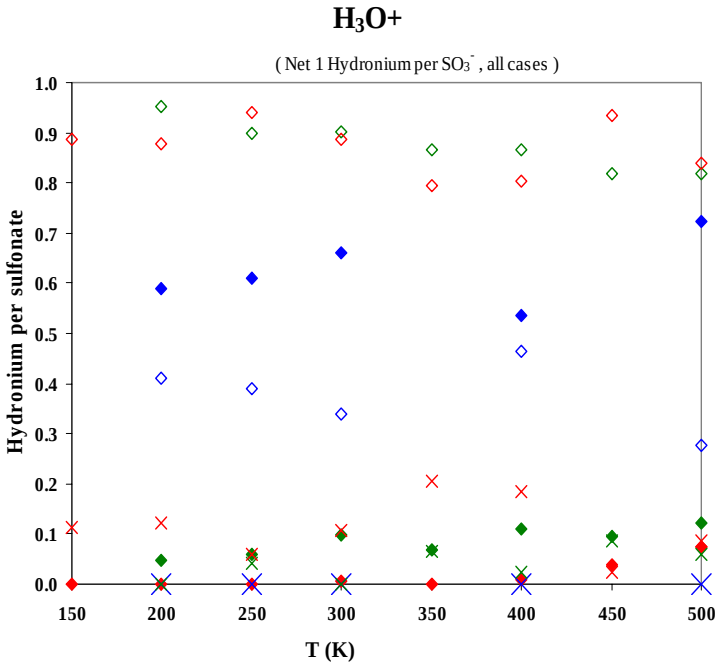

b)

Figure 3. Plots depicting the partition of solvent molecules among bound, loose, and free states for water (a) and hydronium (b) as a function of temperature for Nafion 117.

3.2 Thermal Properties

3.2.1 Thermal expansion. The volume-temperature relations of the respective systems provide measurable properties which can be used as an initial test of force field validity. From Figure 4, it is found that system density decreases with increasing hydration level. Further, from extrapolating the trends in specific volume at the extreme ends of the temperature range, it is found that the indicated glass transition temperature drops from approximately 320K to 300 K as hydration level increased. This trend is presumed to be due to the plasticization provided by the presence of additional water molecules. Because the removal of energy is done over extremely short time scales (e.g., 10^{-8} *K/sec*), actual glass temperatures are expected to be lower. Another feature of volume-temperature relations is that, above the glass transition, the coefficient of thermal expansion increases with increasing hydration while, below the glass transition, it does not.

Because thermal expansion is largely due to an increase in free volume and because it has been speculated that one of the factors which promote weakening is differential nano-scale expansion in the membrane with varying hydration and temperature, a survey of free volume according to zones within the system was performed. These results are shown in Figure 5. Linear fits to some of the data indicate that loose and bound solvent expand by a larger amount than the backbone. This differential expansion may lead to tensile stress in the backbone chains which may in turn promote inter-chain slippage at elevated temperature.

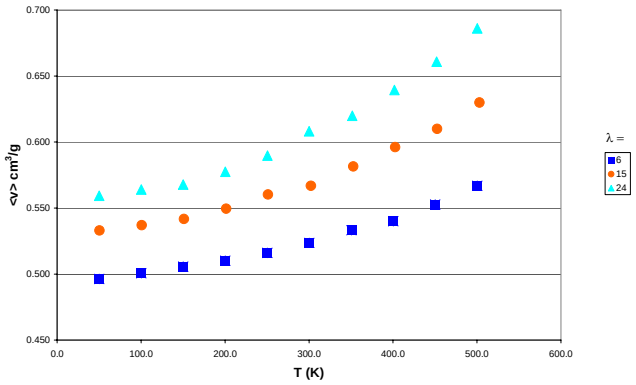

Figure 4. The predicted volume-temperature relation for Nafion-117 for three hydration levels (λ = 6, 15, and 24 solvent molecules/sulfonate)

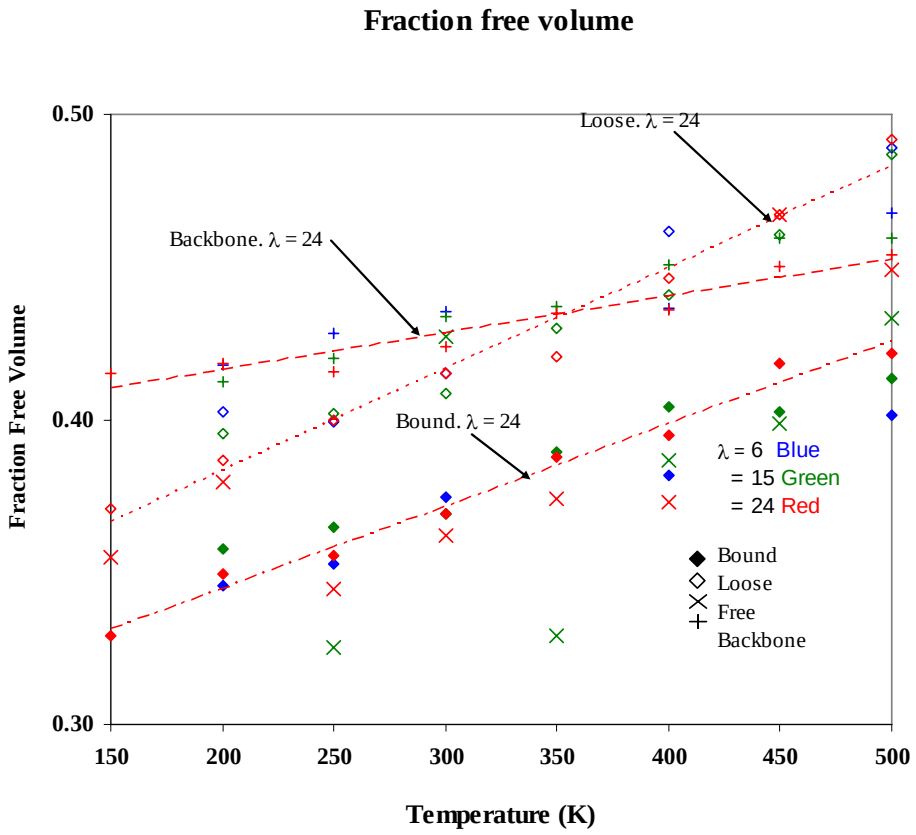

Figure 5. The dependence of free volume fraction as a function of temperature for Nafion-117.

3.3 Geometric Analysis

3.3.1 Atomic Pair Correlation. Pair correlation functions for selected atom pairs over a range of temperature provide insight into how rearrangements and other displacements relate to thermal expansion. Pair correlations for water oxygen atoms, sulfonate sulfur-water oxygen pairs, and sulfonate sulfur-hydronium oxygen pairs are shown in Figures 6 a)-c). When hydration level is low, water appears to be highly ordered with itself and nearly as ordered around sulfonate groups. As temperature rises, these shells become more diffuse and expand to larger radii. The most prominent change with passage across the glass transition temperature is that the hydronium molecules move from primary shells around sulfonates to the secondary shells. A second feature is that, unlike water, there are instances where the hydronium O–sulfonate S pair correlation increases with increasing temperature. At each hydration level, some hydronium appears to have been displaced from the second salvation shell to the inner one. The amount of this displacement increases with increasing hydration level.

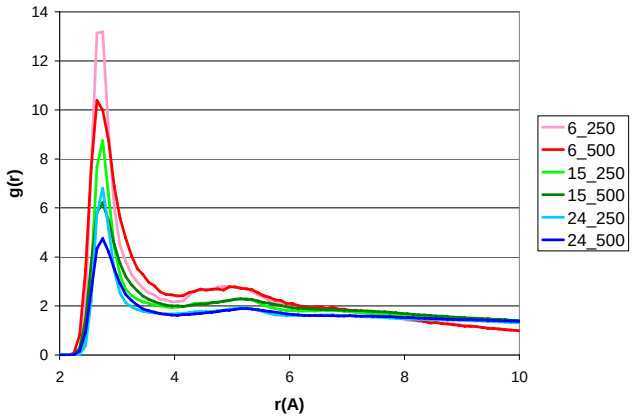

a)

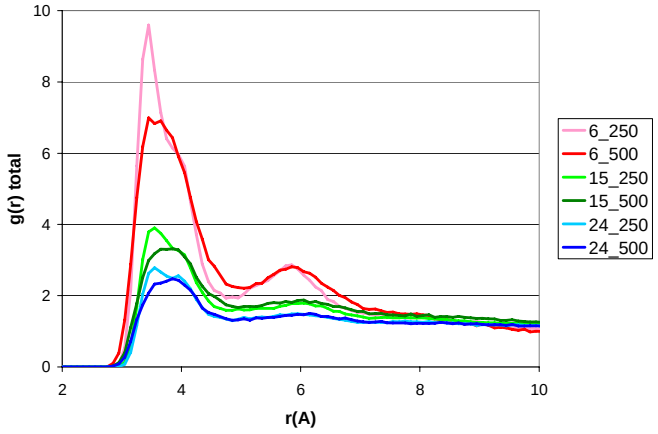

b)

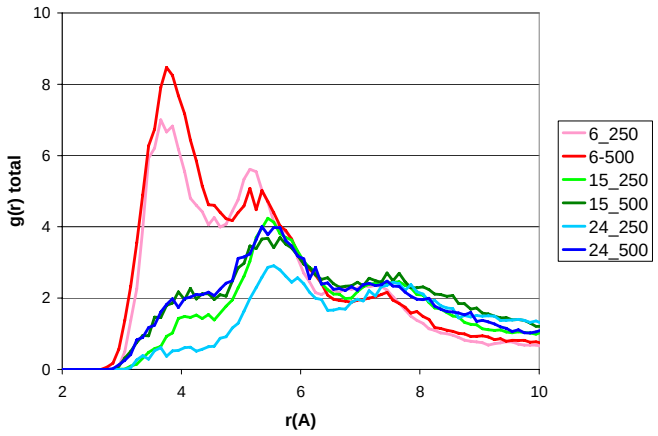

c)

Figure 6. Pair correlation functions for hydrated Nafion-117 systems. Shown are water oxygen (a), sulfonate sulfur – water oxygen (b), and sulfonate sulfur – hydronium oxygen (c). Hydration level (λ) is indicated by the first number in the legend; temperature in Kelvin is indicated by the second.

3.3.2 Atomic Structure Factor. It is thought that the length scales associated with the nano-scale arrangement of solvent molecules in the system is strongly related to proton mobility. Pair correlation functions were used to obtain information about these length scales. The range of scales surveyed is limited to a fraction of the cell size. Structure factor is given by

$$S(q) = 1 + 4\pi \frac{N}{V} \int_0^{\infty} (g(r) - 1) \frac{\sin(q\,r)}{q}\, r\ dr$$

where *N/V* is the number density of the atoms which are surveyed and *g(r)* is the respective pair correlation function. The results for Nafion are given in Figure 7.

There are several notable features in the structure factor spectra. For water, cluster sizes of approximately 11 A were found and these increase with increasing hydration and slightly with increasing temperature. The clustering appears to be most distinct at λ = 15, the intermediate hydration level. For hydronium, increasing temperature had the effect of increasing the distinctness of its clustering; especially for λ = 15. While sulfonate groups were not expected to cluster in the same way as solvent molecules, structure factor nonetheless provides a picture of their arrangement along the solvent channels. Evidence of long range ordering is weak with only a sign of clustering at the lowest hydration level.

3.3.3 Bound solvent orientation. The position and orientation of water, particularly in the bound state, is thought to be an important factor for proton transfer due to positioning for formation of hydrogen bonds as well as solvent dynamics for the vehicular transport of hydrogen. Two studies were performed in this area. In the first, the molecular dynamics force field quality was tested by comparing results from quantum density-functional-theory-based (Q-DFT) predictions for equilibrium solvent position. In the second, the orientation of the bound portion of the solvent population was surveyed.

Minimized zero-temperature molecular dynamics results for the position of a lone water molecule with respect to a sulfonate group showed good agreement with Q-DFT results. In the DISCOVER molecular dynamics environment, a single water molecule was initially positioned in close proximity to sulfonate groups of an SPTES molecule *in vacuo*. The system energy was then minimized. This process was repeated for the various sulfonate groups on the molecule. A rendering of a common equilibrated position is shown in Figure 8. The water dipole vector points toward the sulfonate group and one of the O-S-O planes of the sulfonate nearly coincides with the water H-O-H plane. These results were in close agreement with Q-DFT predictions performed in the GAUSSIAN 2003 environment and using the B3LYP/6-31+G* method and basis sets. The minimized position is shown in Figure 9.

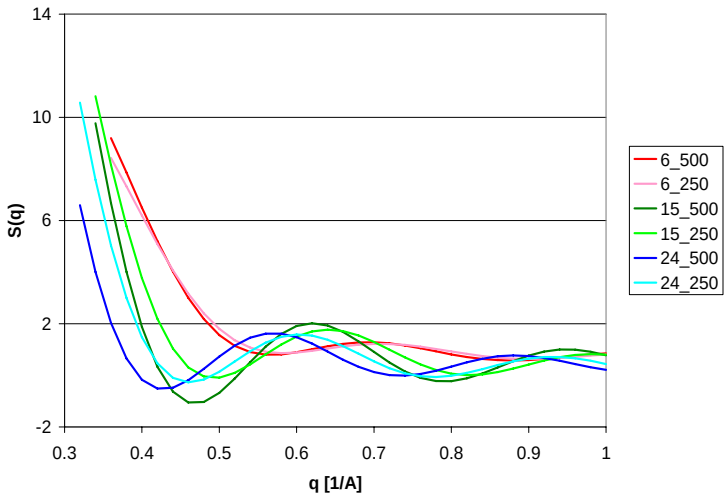

a)

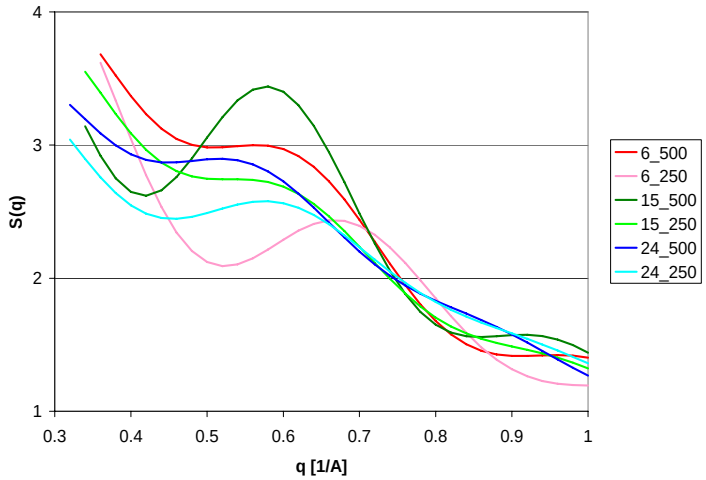

b)

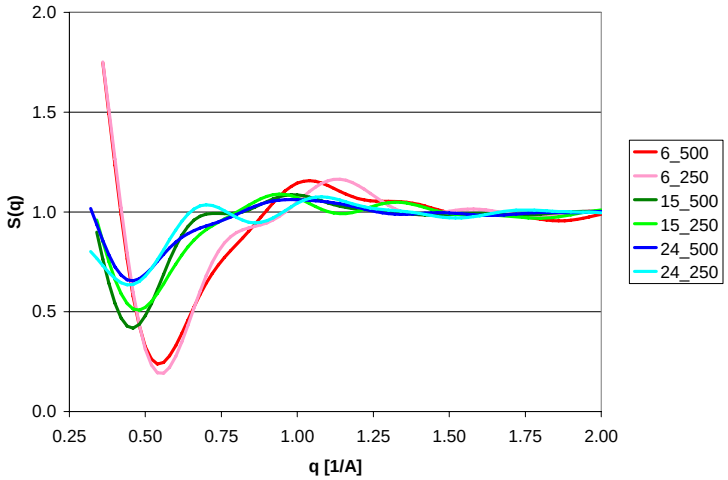

c)

Figure 7. Structure factor functions for water oxygen (a), hydronium oxygen (b), and sulfonate sulfur (c).

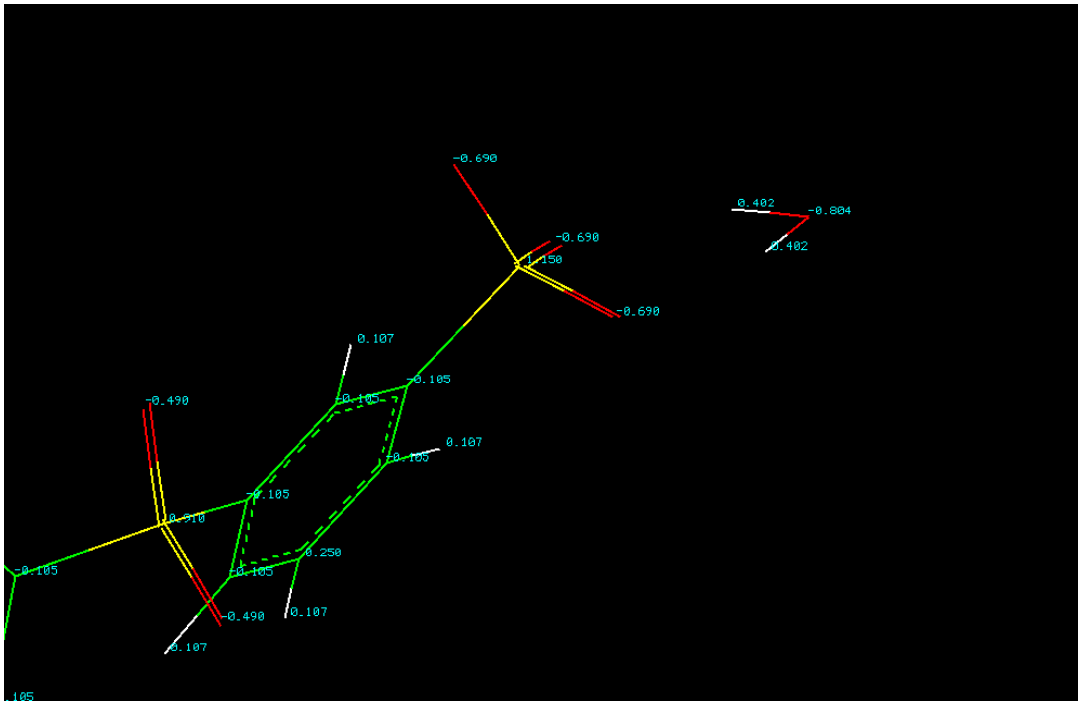

Figure 8. Rendering of the equilibrium position based on the ESFF force field for a lone water molecule with respect to a sulfonate group. The water molecule is in the upper left corner.

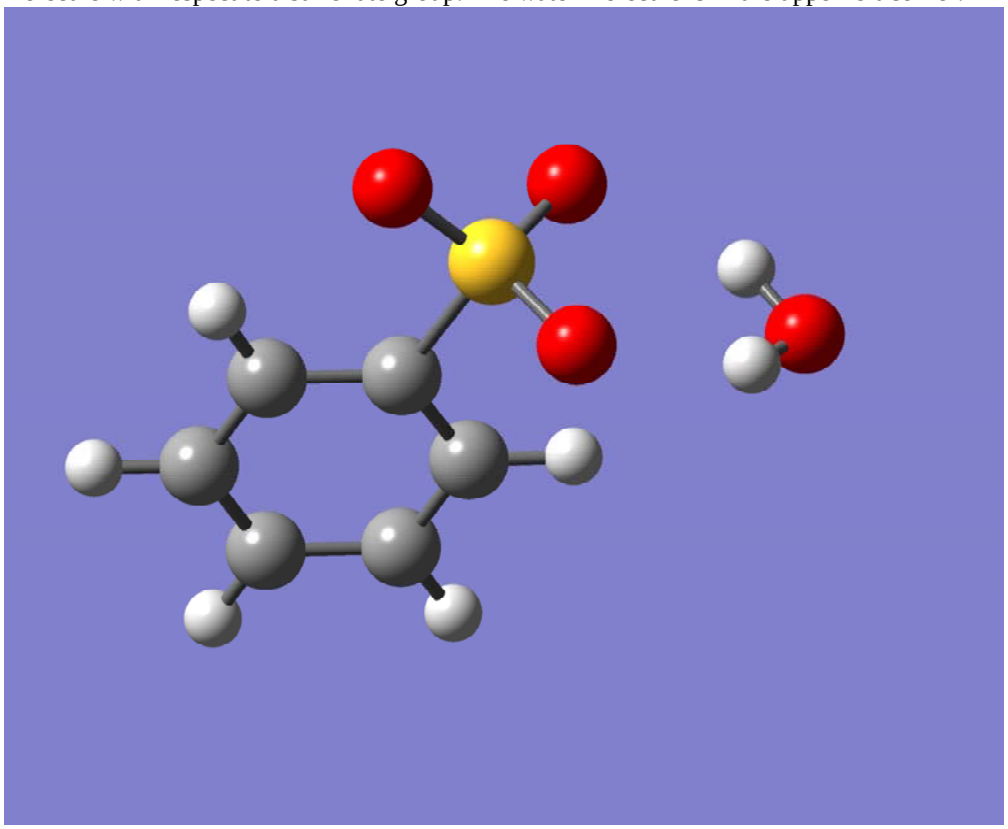
Figure 9. Rendering of the equilibrium position based on the B3LYP/6-31+G* method and basis set for a lone water molecule with respect to phenyl sulfonate.

Additional water-polar group equilibrium positions were predicted and compared. Although its polarity is not as strong as the sulfonate group, the sulfones which connected certain phenyl groups also presented a binding site, apparently due to the steric hindrance it presents to phenyl group rotation. The comparison is shown in Figure 10.

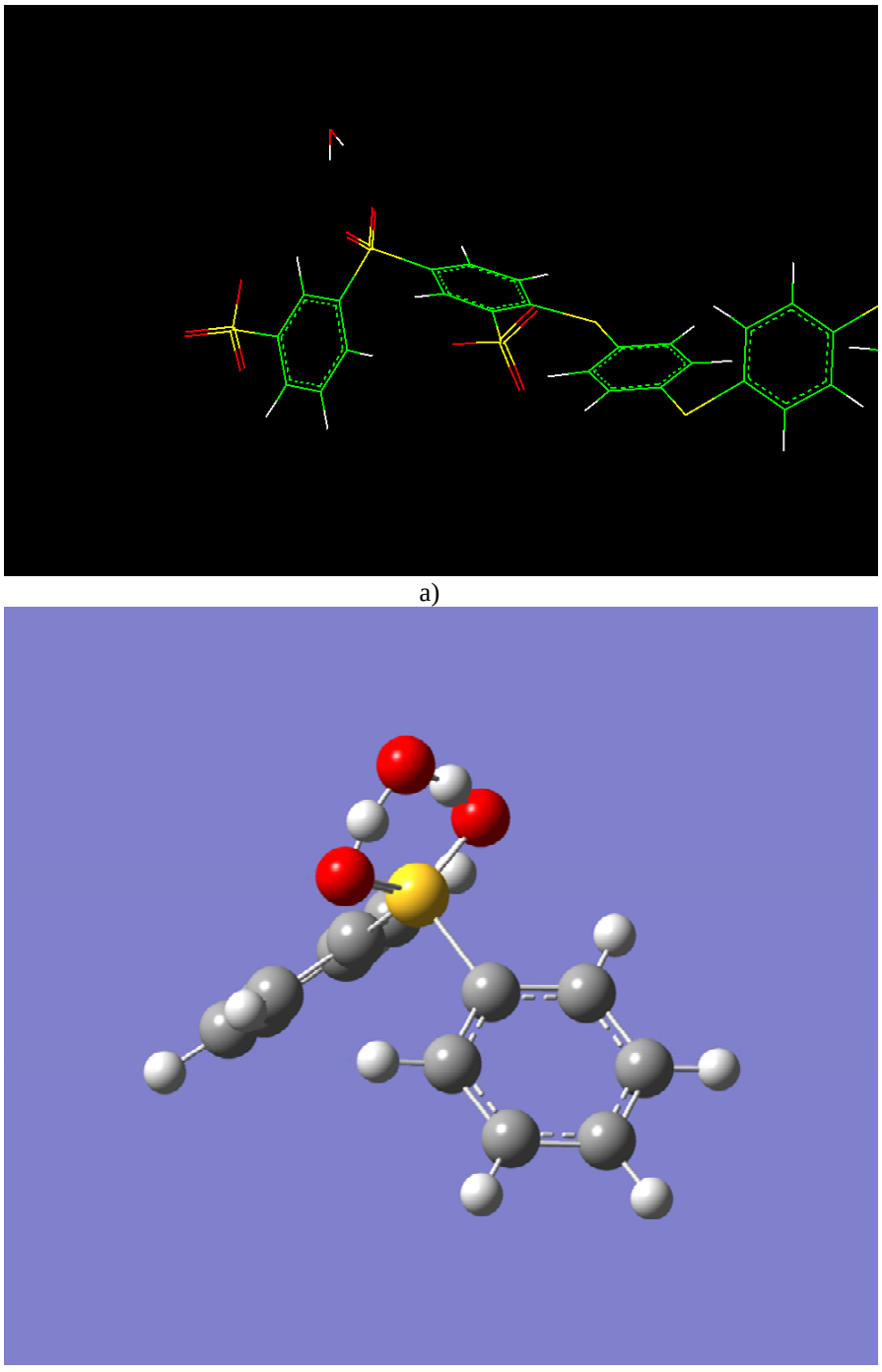

a)

b)

Figure 10. Renderings of the equilibrium position of a lone water molecule with respect to a sulfone group. The result from the ESFF force filed in the DISCOVER environment is shown in a). The result from Q-DFT using B3LYP/6-31+G* is shown in b).

Further minimizations performed in the DISCOVER environment identified additional local minima for water position. These were identified by performing a series of minimizations in which the water molecule was initially positioned close to a different polymer atom in each successive minimization. In certain instances, the water was found to straddle the phenyl group which its hydrogen atoms in proximity to the sulfides at either end of the phenyl. In other cases, water straddled a line between a sulfonate oxygen and a nearby sulfone oxygen. Renderings of these are shown in Figure 11.

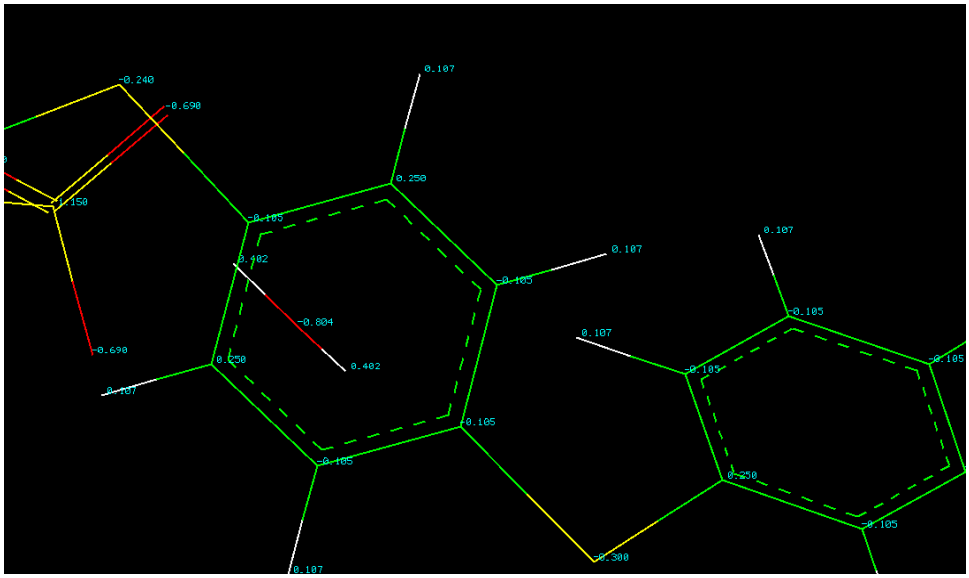

a)

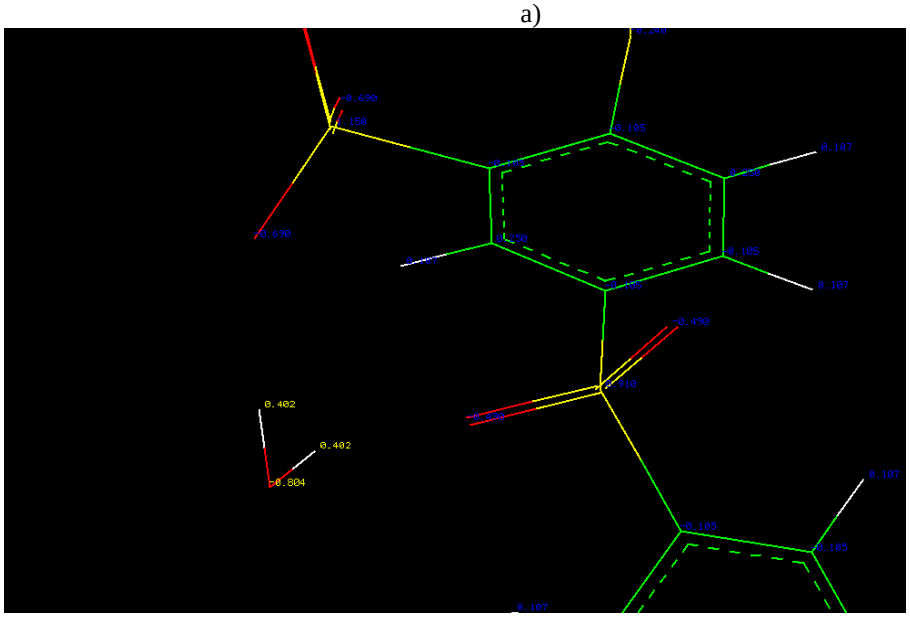

b)

Figure 11. Renderings of water molecules in equilibrium positions in proximity to a phenyl ring (a) and near a neighboring sulfone and sulfonate groups (b).

The foregoing minimized results do not reflect the effects of temperature and additional solvent molecules. The knowledge of water position and orientation was therefore further enhanced by surveying the bound portion of the solvent population from dynamics simulations. As an example, the angle between the bound water dipole and the sulfonate dipole was calculated. A histogram of the results for Nafion at 300 K is shown in Figure 12. From these data, it is observed that the water dipole is essentially never parallel or anti-parallel with the sulfonate dipole but rather has a relatively uniform probability over the range of 45 to 135 degrees. Another quantity calculated was the angle between the sulfonate dipole and the vector from the sulfonate sulfur to the water center-of-mass. This angle represents the azimuthal position of the water in the shell about the sulfonate. The distribution shown in Figure 12 indicates a strong probability for this angle to be approximately 120 degrees. This value is larger than found in the in vacuo zero-temperature results and indicates and indicates the water tends to be positioned backward from the O-S-O planes and away from the sulfonate dipole. It is not yet determined whether the zone more closely coincident with the sulfonate dipole is occupied by free volume or hydronium molecules.

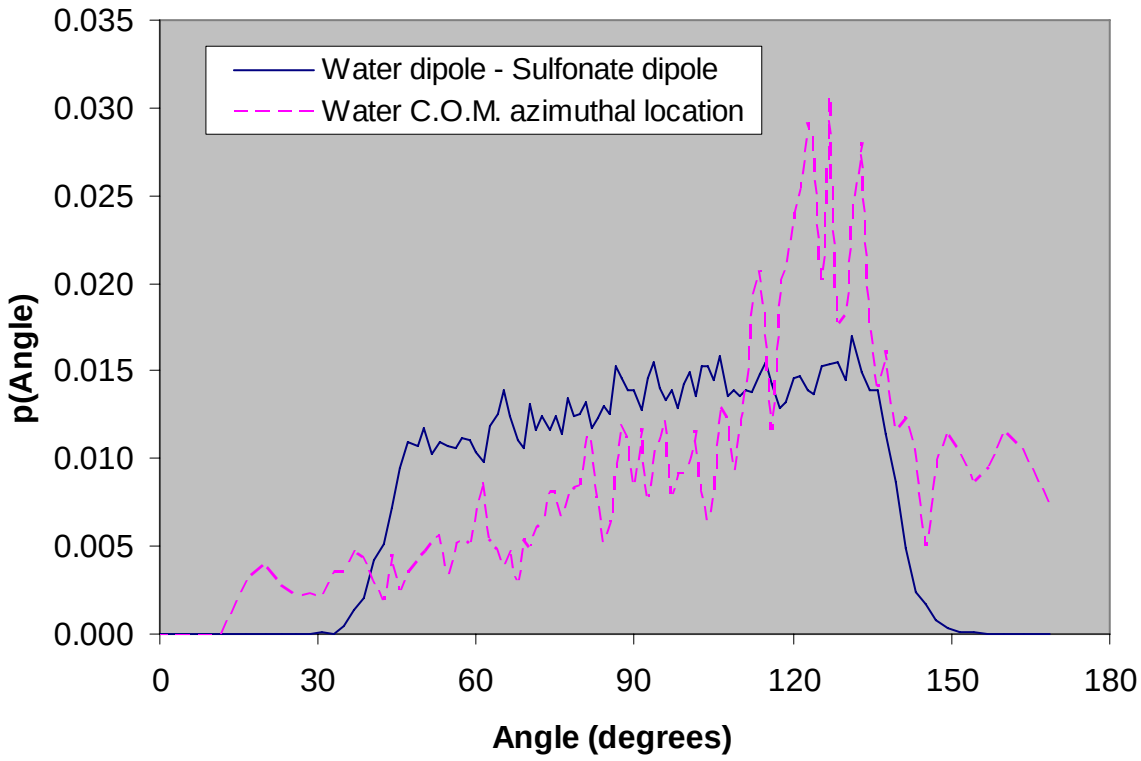

Figure 12. The probability distribution function of the angle between bound water and sulfonate dipoles for Nafion at 300 K.

3.3.4 Hydrogen Bonding. It is well-established that hydrogen bonding is an important factor affecting solvent dynamics and ordering. While the nature of hydrogen bonding in liquid phase water has been studied a great deal, the ways in which the polymer polar groups hydrogen-bond to the solvent and affect solvent-solvent bonding continues to be an area of close scrutiny.

At present, hydrogen bonding among the various hydrogen-bearing species has been surveyed based on geometric criteria. Sulfonate, water, and hydronium oxygen atoms were each treated as being candidate acceptor atoms. Snapshots from dynamics runs were surveyed to find potential donor oxygen – hydrogen pairs within a selected radius (which was set to 3 A). For donors which met this criterion, the donor-hydrogen-acceptor angle was also measured. If this angle was greater than 90 degrees, a hydrogen bond was declared.

A initial survey of O-O distances and D-H-A angles for a Nafion system indicates distinct differences among water, hydronium, and sulfonate as well as among the nature of hydrogen bonding among bound, loose, and free states. The results are shown in Figures 13-16 for distances and angles, respectively.

a)

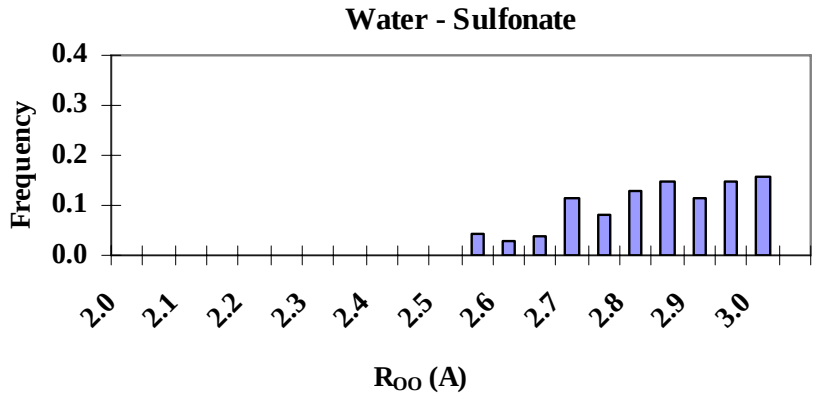

b)

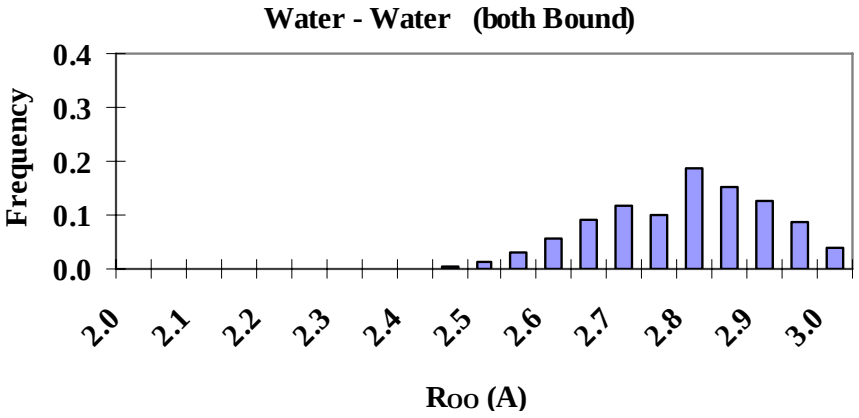

c)

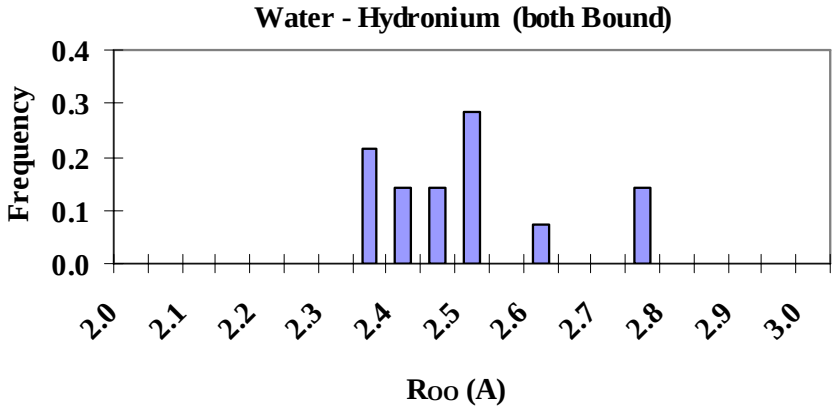

Figure 13. Histograms of O-O and O-S separation distance among selected species populations within the sulfonate first solvation shell. Shown are water O to sulfonate S (a), water O to water O when both are bound (b), water O to hydronium O when both are bound.

a)

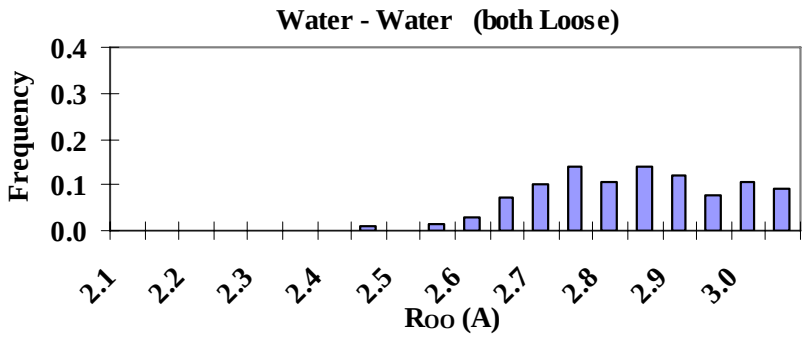

b)

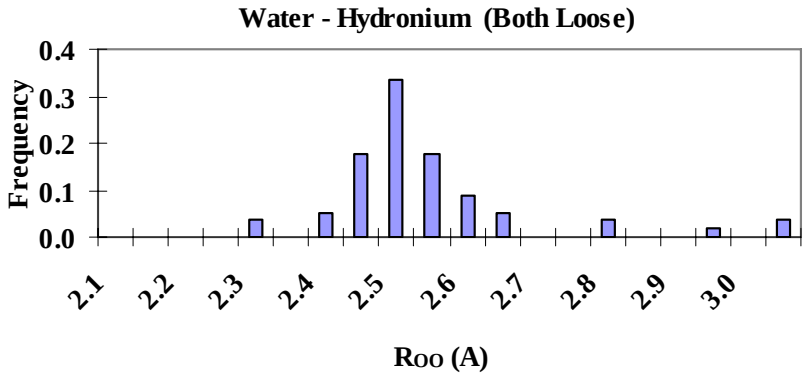

c)

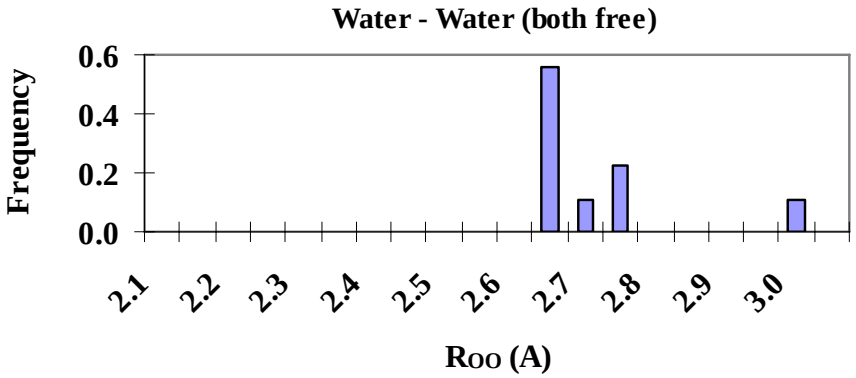

Figure 14. Histograms of O-O separation distance among water and hydronium populations in the free and loosely-bound states. Shown are water O to water O where both are loose (a), water O to hydronium O when both are loose (b), water O to water O when both are free.

a)

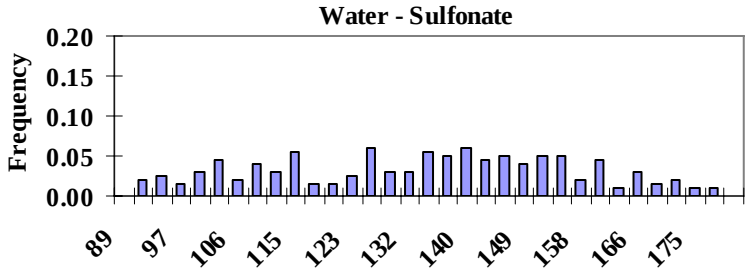

b)

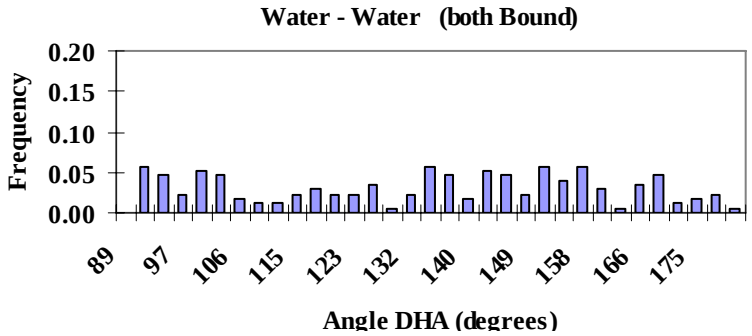

c)

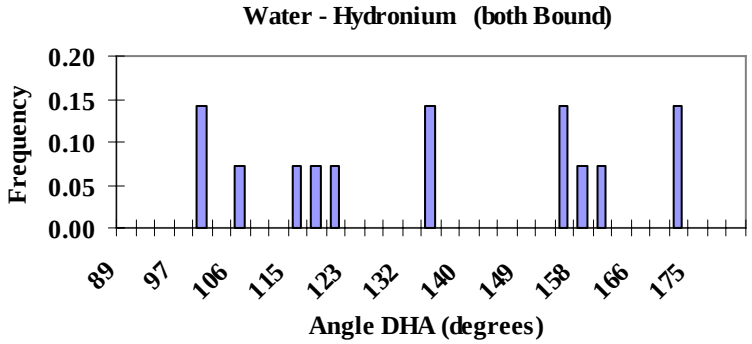

Figure 15. Histograms of donor-hydrogen-acceptor angle among selected species populations within the sulfonate first solvation shell. Shown are water O to sulfonate S (a), water O to water O when both are bound (b), water O to hydronium O when both are bound.

a)

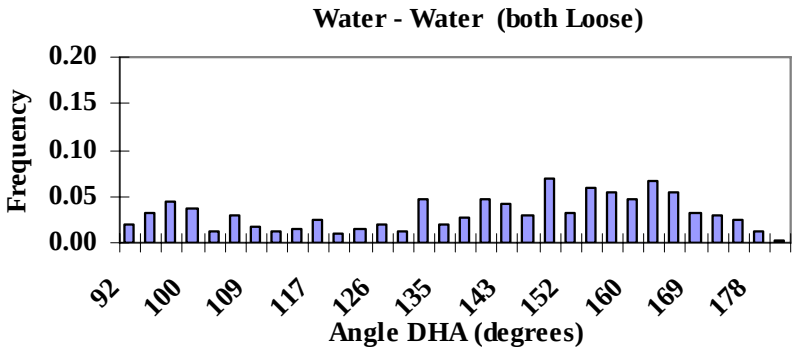

b)

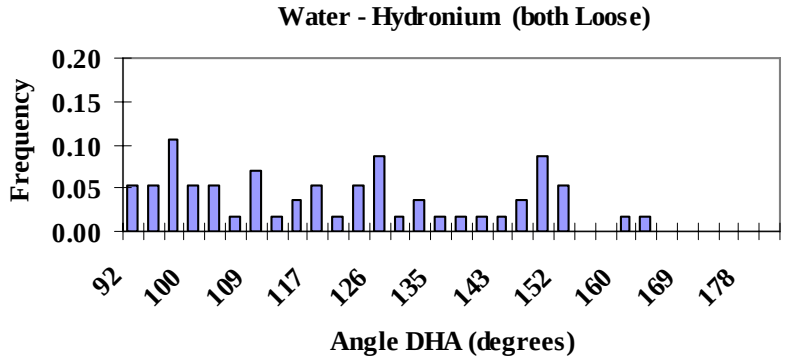

c)

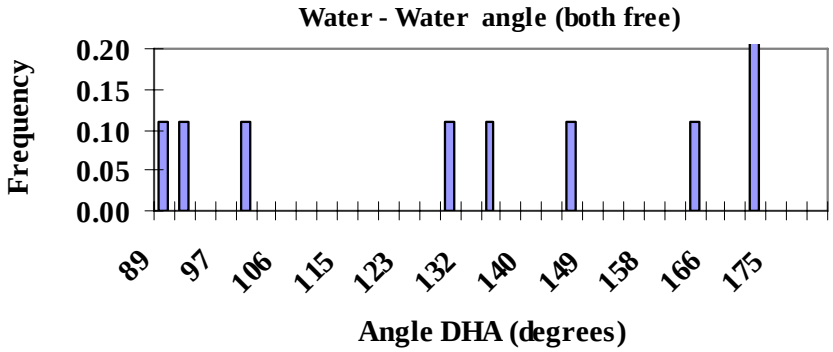

Figure 16. Histograms of donor-hydrogen-acceptor angle among water and hydronium populations in the free and loosely-bound states. Shown are water O to water O where both are loose (a), water O to hydronium O when both are loose (b), water O to water O when both are free.

3.4 Dynamic Analysis

3.4.1 Rotational Diffusion Autocorrelation functions were prepared for both OH and dipole vectors for both water and hydronium. The decay in these can be compared with NMR correlation time measurements. The analysis was performed with the recognition that there may be multiple phenomena occurring; each of which has a different characteristic time. Because

there are commonly multiple factors which affect the decay in the autocorrelation, the results were analyzed to determine the characteristic times which dominate this decay. Examples of such factors include non-bond interaction strength and the mean distance to neighboring molecules.

Another factor which is anticipated to affect rotational decay rate is the proximity of the molecule to polar groups (such as sulfonates and sulfones). To elucidate any differences in behavior based on this proximity, the solvent molecules at each recorded instant in the trajectory were sorted into bound, loosely-bound, and free groups for analysis. Bound solvent was defined as being within the first salvation shell of sulfonate and free solvent was defined as having only unbound solvent as near-neighbors. The balance was defined as loosely-bound. Examples of the autocorrelation function for these groups and the entire population are shown in Figure 17.

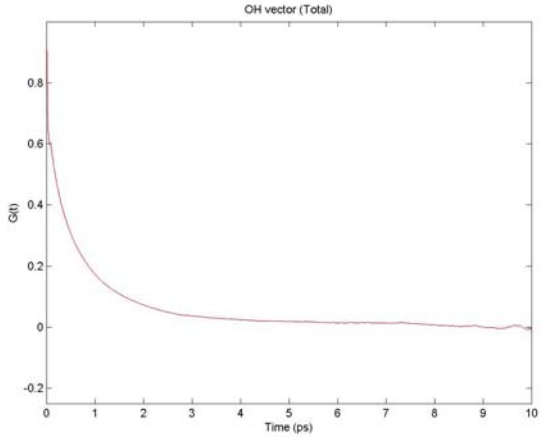

a)

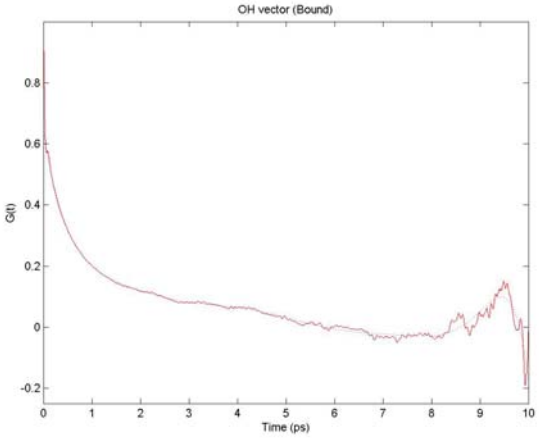

b)

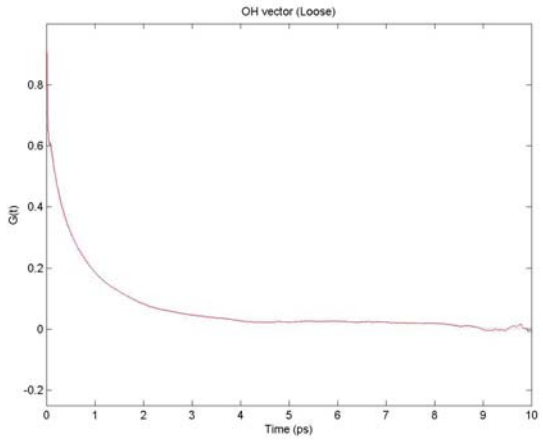

c)

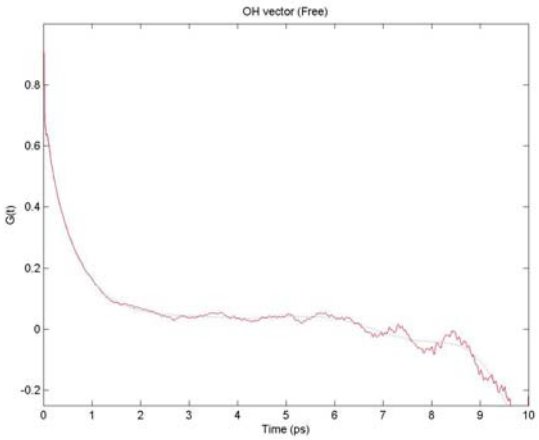

d)

Figure 17. Autocorrelation functions for motion of the OH vector in hydrated Nafion 117 at 300 K with λ = 24. Functions for the total population (a) as well as the bound (b), loosely-bound (c), and free (d) components are shown.

Detailed information about the correlation time scales was obtained by converting autocorrelation functions to the spectral domain. If it is assumed that a function can be represented as a finite series of exponentially-decaying terms, that is

$$G(t) = \sum_{i=}^{n} A_i \exp\left(-t/\tau_i\right)$$

Similarly, if the function is assumed to be an infinite series of terms, *G(t)* can be written (15)

$$G(t) = G_e + \int_{-\infty}^{\infty} H(\tau) \exp\left(-t/\tau\right) d(\ln\tau) \cong G_e + \int_{\ln t}^{\infty} H(\tau) d(\ln\tau)$$

Where $H(\tau)$ is the relaxation spectrum. A first-order estimate of *H(t)* is given by (16)

$$H(\tau) \cong -\left.\frac{d\,G(t)}{d\,(\ln t)}\right|_{t=\tau}$$

Relaxation spectra for water and hydronium molecules highlight the differing sizes and levels of the time constants involved in their motion. Example spectra are shown in Figure 18. Time constants for water are distinctly less than those of hydronium. The behavior of bound molecules differs from those which are loosely-bound; especially for $\tau > 0.14$ ps.

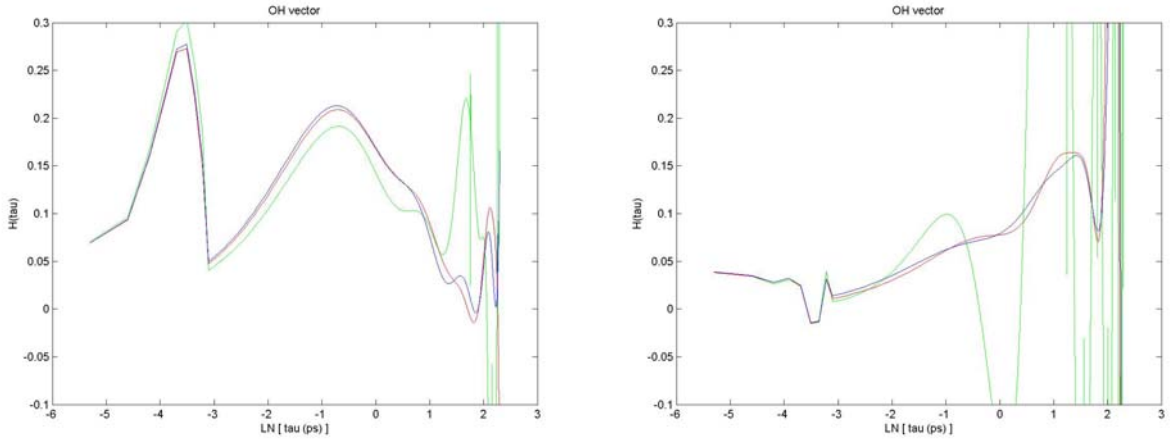

a) b)

Figure 18. The relaxation spectra obtained from the autocorrelation functions for the OH vector of water (a) and hydronium (b) molecules in Nafion-117 at 300 K and λ = 24. Spectra for bound (green), loosely-bound (red), and total (blue) populations are shown.

3.4.2 Velocity Autocorrelation. While the velocity autocorrelation function can be used to estimate self-diffusion coefficient, the short term time-dependence of solvent center-of-mass dynamics can also be studied for the purpose of identifying whether the mean "temperature" associated with motion of the entire solvent molecule differed among bound, loose, and free states and also to investigate whether there is oscillation associated with the solvent motions. Plots of velocity autocorrelation for water are given in Figure 19. The water center-of-mass mean squared velocity is highest for free molecules and lowest for bound.

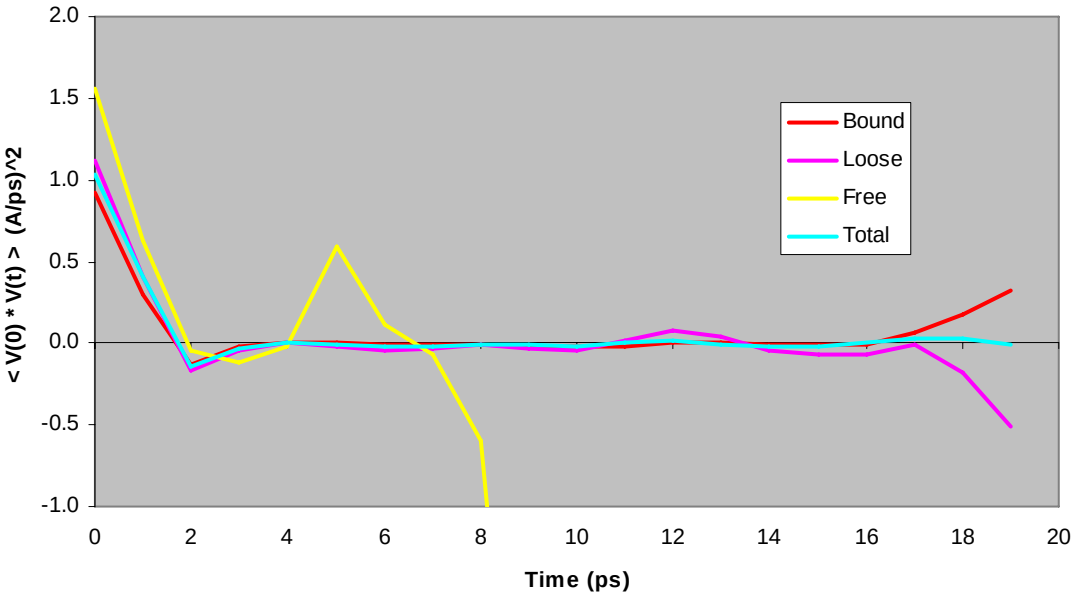

Figure 19. Velocity autocorrelation function for bound, loose, and free water populations in Nafion 117 at 300 K.

Oscillation was examined by Fourier analysis of the velocity autocorrelation function. This is done as follows

$$F(\omega)=\int_0^{\infty}\langle v(t)\bullet v(t+\tau)\rangle\cos(\omega\tau)d\tau$$

The results are shown for an example Nafion system at 300 K in Figure 20. The spectra indicate that there is indeed a strong oscillatory component of the motions of the bound, loose, and free populations because of the peaks and strong harmonics in the spectra. What is also found is that the frequencies of each are different to the extent that the spectrum for the entire population is thoroughly blended and does not depict the unique behaviors among the sub-populations.

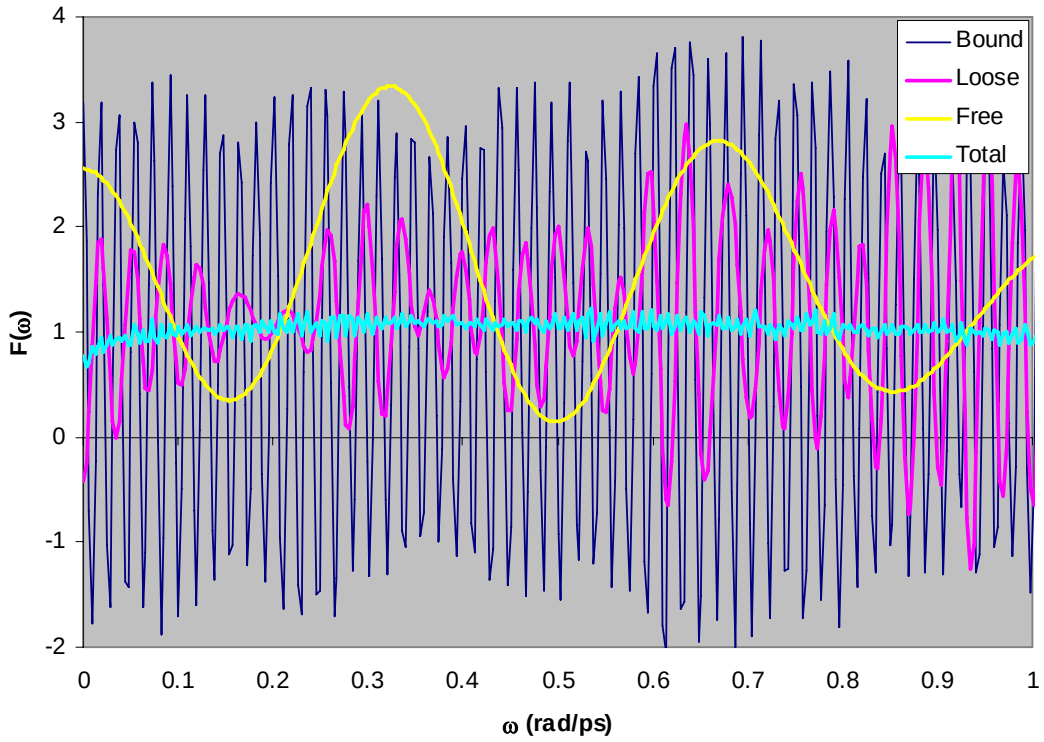

Figure 20. Fourier transform results of velocity autocorrelation functions of water in Nafion 117.

4. CONCLUSIONS

Molecular dynamics simulations have been used to explore the kinetic and geometric features of hydrated polymer systems for use in membranes. Solvent rotational dynamics can be clarified by sorting according to proximity to polar groups and by analysis of relaxation spectra. The reasons for the high conductivity of SPTES at high temperature continue to be explored.

ACKNOWLEDGEMENTS

The author would like to thank Rajiv Berry, Christopher Grote, Martin Schwartz, Peter Mirau, and Nalini Berry for their assistance.

5. REFERENCES

1. K.-D. Kreuer, S.J. Paddison, E. Spohr, and M. Schuster, Chem. Rev., **104**, 4637 (2004).
2. M. Eikerling, S.J. Paddison, L.R. Pratt, and T.A. Zawodzinski, Jr., Chem. Phys. Lett., **368**, 108 (2003).
3. S. Urata, J. Irisawa, A. Takada, W. Shinoda, S. Tsuzuki, and M. Mikami, J. Phys. Chem. B, **109**, 4269 (2005).
4. S.S. Jang, V. Molinero, T. Cagin, and W.H. Goddard III, J. Phys. Chem. B, **108**, 3149 (2004).
5. G. Gebel, and L. Lambard, Macromolecules, **30**, 7914 (1997).
6. G. Gebel, Polymer, **41**, 5829 (2000).
7. K.-D. Kreuer, J. Membrane Sci., **185**, 29 (2001).
8. M. Eigen, L. De Maeyer, Proc. Royal Soc. (London), Ser. A, **247**, 505 (1958).
9. M. Eigen, Agnew. Chem., **75**, 489 (1963).
10. S. Urata, J. Irisawa, A. Takada, S. Tsuzuki, W. Shinoda, and M. Mikami, Phys. Chem. Chem. Phys., **6**, 3325 (2004).
11. Z. Bai, M.F. Durstock, and T.Y. Dang, J. Membrane Sci., **281**, 508 (2006).
12. M. Schuster, K.-D. Kreuer, H.T. Andersen, and J. Maier, Macromolecules, **40**, 598 (2007).
13. S. Shi, L. Yan, Y. Yang, J. Fisher-Shaulsky, and T. Thacher, J. Comput. Chem., **24**, 1059, (2003).
14. N.J. Bunce, S.J. Sondheimer, and C.A. Fyfe, Macromolecules, **19**, 333 (1986).
15. J.D. Ferry, Viscoelastic Properties of Polymers, 3rd ed., John Wiley & Sons, New York, 1980, pg. 81.
16. T. Alfrey and P. Doty, J. Appl. Phys., **16**, 700 (1945).